X-ray emission from T Tauri stars

M. Jardine, A. Collier Cameron, J.-F. Donati, S. G. Gregory, K. Wood

Mon. Not. R. Astron. Soc. **367,** 917–927 (2006) doi:10.1111/j.1365-2966.2005.09995.x

X-ray emission from T Tauri stars

M. Jardine,[1⋆] A. Collier Cameron,[1] J.-F. Donati,[2] S. G. Gregory[1] and K. Wood[1]

[1]*SUPA, School of Physics and Astronomy, University of St. Andrews, St. Andrews KY16 9SS*
[2]*Laboratoire dAstrophysique, Observatoire Midi-Pyrénées, 14 Av. E. Belin, F-31400 Toulouse, France*

Accepted 2005 December 20. Received 2005 December 16; in original form 2005 November 17

ABSTRACT

We have modelled the X-ray emission of T Tauri stars assuming that they have isothermal, magnetically confined coronae. These coronae extend outwards until either the pressure of the hot coronal gas overcomes the magnetic field, or, if the corona interacts with a disc before this happens, by the action of the disc itself. This work is motivated by the results of the *Chandra* Orion Ultradeep Project that show an increase in the X-ray emission measure (EM) with increasing stellar mass. We find that this variation (and its large scatter) results naturally from the variation in the sizes of the stellar coronae. The reduction in the magnitude of the X-ray emission due to the presence of a disc stripping the outer parts of the stellar corona is most pronounced for the lower mass stars. The higher mass stars with their greater surface gravities have coronae that typically do not extend out as far as the inner edge of the disc and so are less affected by it. For these stars, accretion takes place along open field lines that connect to the disc. By extrapolating surface magnetograms of young main-sequence stars, we have examined the effect on the X-ray emission of a realistic degree of field complexity. We find that the complex fields (which are more compact) give densities of some (2.5–0.6) $\times$ 10^{10} cm^{-3}. This is consistent with density estimates of (1–8) $\times$ 10^{10} cm^{-3} from modelling of individual flares. A simple dipole field in contrast gives densities typically an order of magnitude less. For the complex fields, we also find surface hotspots at a range of latitudes and longitudes with surface-filling factors of only a few per cent. We find that the dipolar fields give a relationship between X-ray EM and stellar mass that is somewhat steeper than observed, while the complex fields give a relation that is shallower than observed. This may suggest that T Tauri stars have coronal fields that are slightly more extended than their main-sequence counterparts, but not as extended as a purely dipolar field.

Key words: stars: activity – stars: imaging – stars: pre-main-sequence – stars: rotation – stars: spots.

1 INTRODUCTION

The recent *Chandra* Orion Ultradeep Project (COUP) has provided a remarkable data set of the X-ray emission of pre-main-sequence stars. It shows that for these T Tauri stars (as for main-sequence field stars), the X-ray emission measure (EM) rises slowly with stellar mass. For the T Tauri stars that show signs of active accretion, however, the correlation is less well defined (Preibisch et al. 2005). These COUP stars have rotation rates (or Rossby numbers) that place them in the *saturated* or *supersaturated* part of the X-ray emission–rotation rate relation, but with EMs slightly below those of their main-sequence counterparts. This suppression of the X-ray emission also appears to be related to the presence of active accretion from the surrounding disc. The detection of significant rotational modulation in some of the saturated stars suggests that the saturation of the X-ray emission is not the result of the complete coverage of the stellar surface in emitting regions (Flaccomio et al. 2005). Rather, the emitting regions must be distributed unevenly around the star and they do not extend significantly more than a stellar radius above the surface.

Observations of flares also yield information about the structure of T Tauri coronae. Although flares typical of the compact flares seen in main-sequence stars have been observed in the COUP sample, extremely large flares have also been detected. Estimates of plasma densities based on these flare observations are in the range of (1–8) $\times$ 10^{10} cm^{-3} (Favata et al. 2005). The derived lengths of the flaring loops are around the location of the corotation radius ($5R_\star$) for the most reliable estimates, although some loop lengths appear to be much greater, suggesting perhaps that these flares have taken place in loops that link the star and the surrounding disc.

⋆E-mail: moira.jardine@st-and.ac.uk

The X-ray data from COUP therefore suggest that T Tauri stars have coronae that are structured on a variety of length-scales, ranging from compact loops on scales of a stellar radius to much longer structures on the scale of the inner regions of an accretion disc. Observations of T Tauri magnetic fields also point to a very complex field structure, with localized regions of high field strength on the stellar surface. Unpolarized Zeeman-splitting measurements for photospheric lines with high Lande g-factors typically yield field strengths on T Tauri stars of the order of 2–3 kG (Johns-Krull, Valenti & Koresko 1999; Johns-Krull, Valenti & Saar 2004), with surface-filling factors of the order of some tens of per cent. Similarly, the observed splittings of the circularly polarized Zeeman σ components in the He I 5876 line indicate that the accretion streams impact the stellar surface in regions where the strength of the local magnetic field is of the order of 3–4.5 kG (Guenther et al. 1999; Johns-Krull et al. 1999; Symington et al. 2005). As Valenti & Johns-Krull (2004) pointed out, unpolarized Zeeman-broadening measurements are sensitive to the distribution of magnetic field strengths over the stellar surface, but yield little spatial information. Circular polarization methods such as Zeeman–Doppler imaging give better spatial information about the magnetic polarity distribution, but have limited ability to determine field strengths at the level of the photosphere.

The rate at which the field strength declines with radial distance from the star depends on the complexity of the magnetic polarity distribution on the stellar surface. On the Sun, much of the flux emerging from small-scale bipolar regions in the photosphere connects locally to nearby regions of opposite polarity. The locally connected field lines do not contribute to the coronal field at heights greater than the footpoint separation. As a result, the power-law dependence of the average coronal field on height steepens with increasing field complexity. A simple model assuming a global dipole with a surface field strength of the order of 2–3 kG would probably assume too high a value for the surface field, and allow it to decline too slowly with radial distance.

Zeeman–Doppler images of post-T Tauri stars give us a much better idea of the complexity of the magnetic field, and hence of the rate at which it falls off with height. The surface resolution of a Zeeman–Doppler image is determined by the ratio of the star's rotational line broadening to that of the intrinsic line profile convolved with the instrumental resolution. On length-scales smaller than a resolution element, the circular polarization signals from small-scale field concentrations of opposite polarity cancel. The Zeeman broadenings seen in unpolarized light, however, do not. The 'field strengths' in Zeeman–Doppler images are in effect magnetic flux densities, averaged over a surface resolution element (Donati & Collier Cameron 1997). For this reason, the highest flux densities seen in Zeeman–Doppler images are always less than the maximum field strengths determined from unpolarized Zeeman splittings. Potential field extrapolations from Zeeman–Doppler images should give a realistic measure of the field strength as a function of height beyond a few tenths of a stellar radius above the photosphere.

The X-ray coronae of these pre-main-sequence stars appear therefore to display a degree of spatial complexity and activity that is similar to that of their very active (saturated or supersaturated) main-sequence counterparts, but with some significant differences. These differences (the suppression of X-ray emission and the greater scatter in the L_x–$M_\star$ relation) appear to be related to the presence of active accretion. For main-sequence stars, the observed variation with rotation rate of both the magnitude of the X-ray emission and its rotational modulation can be explained by the centrifugal stripping of the outer parts of the corona (Unruh & Jardine 1997; Jardine & Unruh 1999; Jardine 2004). This becomes important once the star is rotating sufficiently rapidly that its corotation radius is within the corona. Ivanova & Taam (2003) have shown that this process can also reduce the angular momentum loss rate of rapid rotators (relative to more slowly rotating stars) without requiring a saturation of dynamo activity at high rotation rates. While most T Tauri stars are not rapidly rotating, their lower surface gravities and therefore greater pressure scaleheights mean that their coronae may be more extended than their main-sequence counterparts. This suggests that a similar process may be important for these stars too. The presence of active accretion from the inner edge on an accretion disc may distort the corona of a T Tauri star, leading to a similar (but additional) stripping effect.

The aim of this paper is to model the X-ray emission from T Tauri stars, using the data (masses, radii, rotation periods, X-ray EMs and temperatures) provided by the COUP results (Getman et al. 2005). We show these apparently puzzling features of X-ray emission from T Tauri stars can be explained in the context of the varying sizes of stellar coronae that are limited either by the gas pressure of the stellar corona or by the presence of a disc.

2 SIMPLE MODEL

2.1 Passive disc

We begin by addressing the question: what is the extent of the star's corona? We consider first the situation where each star has a disc that is *passive* in the sense that it does not distort the star's magnetic field. The coronal extent can then be estimated by calculating the height at which the gas pressure begins to exceed the magnetic pressure. In order to do this, however, we need a model for the star's magnetic field structure. As a simple example, we take a dipolar field geometry (see Fig. 1) for which

$$B_r = \frac{2m\cos\theta}{r^3}, \tag{1}$$

$$B_\theta = \frac{m\sin\theta}{r^3}. \tag{2}$$

If we assume that the gas that is trapped on each closed field line is isothermal and in hydrostatic equilibrium then the gas pressure is $p = p_0 \mathrm{e}^{m/kT\int g_s \mathrm{d}s}$ where $g_s = (\boldsymbol{g}\cdot\boldsymbol{B})/|\boldsymbol{B}|$ is the component of gravity along the field. Here, for a star with rotation rate ω,

$$g(r,\theta) = (-GM_\star/r^2 + \omega^2 r\sin^2\theta, \omega^2 r\sin\theta\cos\theta). \tag{3}$$

The gas pressure at the footpoint of the field line p_0 is a free parameter of this model. For this initial simple analysis, we choose to scale this to the magnetic pressure of the average surface field strength $B_0 = \langle|B|\rangle$ such that $p_0 = KB_0^2$ where K is a constant that is the same on every field line. By scaling K up or down, we can scale the overall level of the coronal gas pressure and hence the density and EM (see Appendix A for the calculation of the EM and the density). For each value of K, we can also determine the variation of the gas pressure along each field line and hence the height beyond which the gas pressure exceeds the magnetic pressure. We show in Fig. 1 the *last closed field line*, that is, the most extended field line that can still contain coronal gas. Since the flux function

$$A = \frac{\sin^2\theta}{r} \tag{4}$$

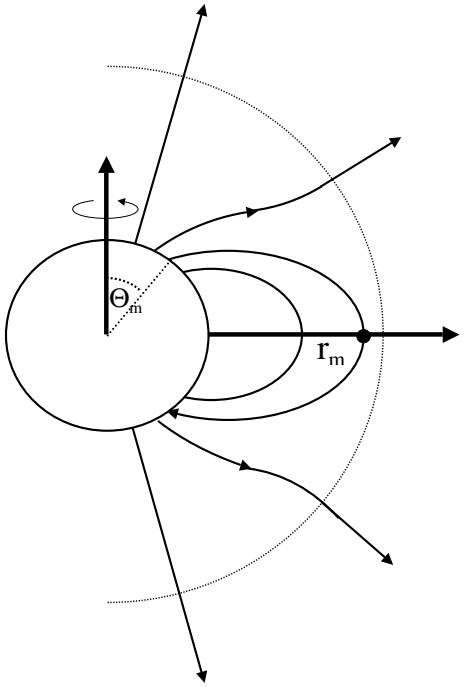

Figure 1. Magnetic structure of a dipole field that has been distorted by the outward pressure of the hot coronal gas trapped on the field lines. Beyond some radius (shown dotted), the pressure of the hot coronal gas is large enough to force open the magnetic field lines. An example is shown of the *last closed field line* that intersects the equatorial plane at a radial distance $r_{\rm m}$ and emerges from the stellar surface at a colatitude $\Theta_{\rm m}$. If the coronal temperature and hence pressure is increased, or the stellar field strength is decreased, then $r_{\rm m}$ moves inwards and the angle $\Theta_{\rm m}$ increases. As a result, the fraction of the stellar surface that is covered in closed field capable of confining X-ray emitting gas decreases.

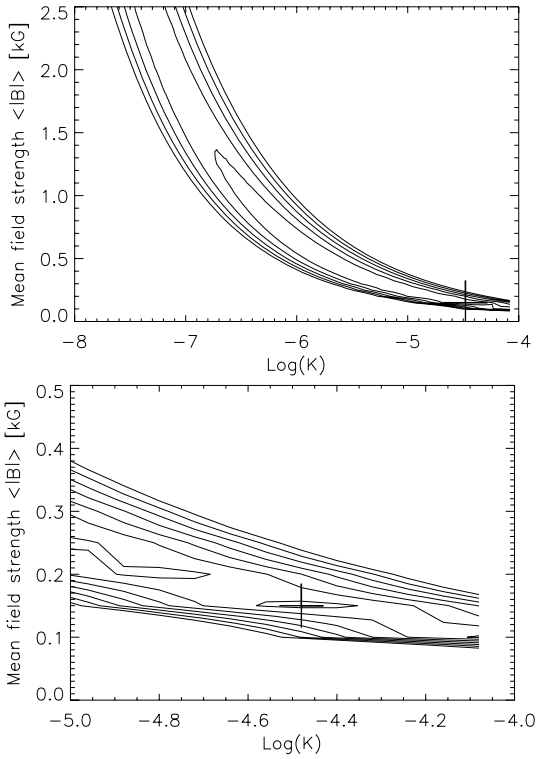

Figure 2. Contours of D (a measure of the goodness of fit to the COUP EMs) as a function of the average value of the magnitude of the surface field strength and the constant of proportionality K which determines the pressure p_0 at the base of the corona since $p_0 = KB_0^2$. The cross marks the position of the minimum value of D and the lower panel shows in greater detail the area around this minimum. The plot shown is for models of the higher temperature EMs. A plot for the lower temperature EMs is qualitatively similar.

is constant along field lines, if this field line crosses the equator at $r = r_{\rm m}$, then it has a footpoint on the stellar surface at a colatitude $\Theta_{\rm m}$ given by

$$\sin^2 \Theta_{\rm m} = \frac{r_\star}{r_{\rm m}}. \quad (5)$$

If the field strength is decreased, or the temperature is increased, then the extent of the last closed field line will decrease and so $\Theta_{\rm m}$ will increase. Our model now has six parameters: the mass, radius and rotation rate of the star, the coronal temperature and the values of the magnetic and gas pressures at the base of the corona. For a large number of stars in the COUP sample the masses, radii and rotation rates have been determined. A two-temperature fit to the X-ray spectra then gives EMs at two different temperatures. This leaves only the base gas and magnetic pressures undetermined. The value of p_0 is simply a scaling factor that raises or lowers the overall coronal pressure. We have chosen to make it proportional to the magnetic pressure since this gives a good agreement between predicted and observed values for EMs and mean densities of both the Sun and other main-sequence stars (Jardine, Collier Cameron & Donati 2002a; Jardine et al. 2002b). We can then simply ask which combination of (p_0, B_0^2) gives the best fit to the EMs of the stars in the COUP sample. To do this, we select 116 stars from the COUP sample for which there are stellar radii, masses and rotation periods (Getman et al. 2005). We exclude one star for which the apparent corotation radius is less than the stellar radius. For each star, we then determine (for each of the two coronal temperatures quoted in the COUP sample) the EM and calculate, for the N stars

$$D = \sum_{i=1}^{i=N} \frac{[\log_{10}({\rm EM}_{{\rm obs},i}) - \log_{10}({\rm EM}_{{\rm calc},i})]^2}{\sigma_i^2}, \quad (6)$$

where the σ_i are the errors in the $\log_{10}$(EM) values. We show in Fig. 2 contours of D for a range of values of (p_0, B_0^2). Clearly, as we choose higher values of the base field strength (which will tend to give a larger corona) we need to have smaller values of the pressure (and hence the density) to give the same EM. Table 1 shows the values of (p_0, B_0^2) that give the best fit to the data and Fig. 3 shows both the observed and calculated EM for these values. Even this simple model reproduces reasonably well the variation of EM with stellar mass and the degree of scatter at each value of $M_\star$. For every value of $M_\star$, there are of course many possible combinations of

Table 1. This shows, for a dipole field, the values of the average field strength $B_0 = \langle |B| \rangle$ at the base of the corona and the corresponding gas pressure $p_0 = KB_0^2$ that give the best fit to the observed EMs from the COUP sample. By fitting relationships of the form (EM) $\propto M_\star^a$ and $\bar{n}_{\rm e} \propto M_\star^b$ to the calculated values of the EMs and densities, we have determined the values of a and b.

	Passive disc		Active disc	
T	High	Low	High	Low
$\langle \lvert B \rvert \rangle$ (G)	100	50	150	50
p_0 (dyne cm^{-2})	1.9	1.2	7.5	1.4
a	0.34	0.38	0.70	0.62
b	−0.09	−0.10	−0.16	−0.16

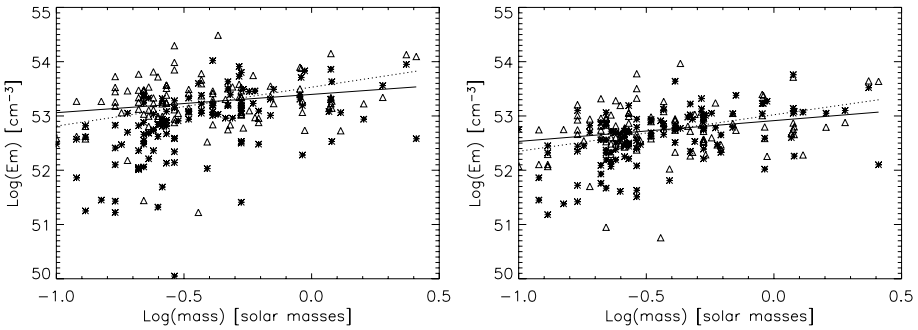

Figure 3. EMs for both the high-temperature (left-hand panel) and low-temperature (right-hand panel) ranges from the COUP sample. Crosses show the observed values while triangles show the values calculated for a dipole field with values of the base magnetic and plasma pressures that give the best fit to the data. For each star, we assume that any disc that may be present is *passive* in the sense that the maximum extent of the corona is limited only by the ability of the magnetic field to contain the hot coronal gas. The solid line is the best fit to the calculated values, while the dotted line is the best fit to the observed values, assuming the errors quoted for the values of log(EM).

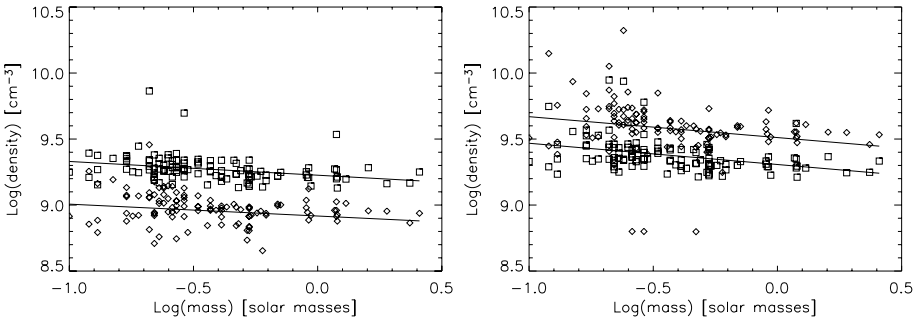

Figure 4. Calculated EM-weighted densities for both the high-temperature (diamonds) and low-temperature (squares) ranges. In the left-hand panel, it has been assumed that any discs that may be present are *passive* so that the size of the corona is limited only by the ability of the magnetic field to contain the hot coronal gas. The right-hand panel, in contrast, shows the densities obtained by assuming that the same stars each have instead an *active disc* so that the extent of the corona is limited by the action of the disc truncating the corona at the corotation radius. The lines show the best fits to the calculated densities.

the other parameters ($R_\star$, $P_{\rm rot}$, T) that determine the extent of the corona and the EM. If we fit a relationship of the form (EM) $\propto M^a_\star$ to the calculated EMs, we find that the slopes in both the high- and low-temperature ranges are shallower than for a corresponding fit to the data, which are, respectively, 0.68 and 0.65 [assuming the errors quoted for the values of log(EM)]. We remind the reader at this point that we are using only a subset of the stars from the COUP survey. We have restricted ourselves only to those that, in addition to EMs and coronal temperatures, also have published masses, radii and rotation periods. For this subset of stars, the slope of the observed EM–mass relation is shallower than we would find if we were to use the full sample of EMs.

We can also (for each of the two temperatures quoted in the COUP data base) calculate the EM-weighted density

$$\bar{n}_{\rm e} = \frac{\int n_{\rm e}^3 \, {\rm d}V}{\int n_{\rm e}^2 \, {\rm d}V} \tag{7}$$

(see Fig. 4). If we fit a relationship of the form $\bar{n}_{\rm e} \propto M^b_\star$ to the calculated EM-weighted densities, we find that the slopes at both the temperature ranges are similar, but the magnitude of the density for the lower temperature range is systematically lower. As shown in the left-hand panel of Fig. 4, these are rather lower than the values of (1–8) $\times$ 10^{10} cm^{-3} determined by Favata et al. (2005) from modelling flares observed in the COUP study, and indeed these are also lower than the values of 10^{10}–10^{13} cm^{-3} calculated for young main-sequence stars (for a comprehensive review see Güdel 2004).

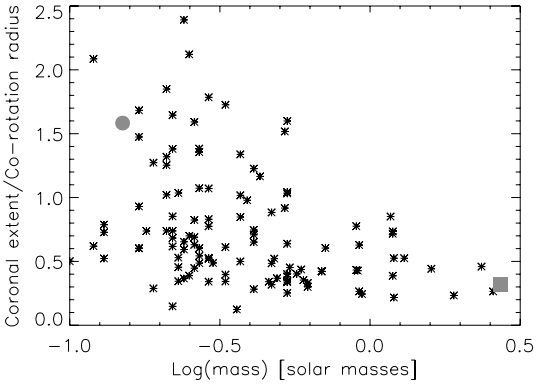

Figure 5. Coronal extent (in units of the Keplerian corotation radius) as a function of stellar mass for stars in the COUP sample. Two stars (marked with a circle and a square) have been selected as examples. Their coronal structure is shown more fully in Figs 8 and 9.

Fig. 5 shows the coronal extents (in units of the corotation radius for each star) that gave this best-fitting value of (p_0, B_0^2). The more massive stars typically have coronae whose extents (relative to their corotation radii) are smaller than that of the lower mass stars. Indeed, for these field strengths and pressures, many of the higher mass stars have coronae that do not extend as far as the corotation radius. It is the lower mass stars with their lower surface gravity that are more likely to have coronae that extend out beyond the corotation radius

and hence to suffer more interaction with any discs that may be present. This may have significant implications for the nature of the interaction between the stellar field and the disc and the exchange of torques between them, since for these higher mass stars it may well be that the disc intercepts not the closed (dipolar) field of the star, but the open field of its wind.

2.2 Active disc

Up to this point, we have considered only the situation where each star has a *passive* disc. Each star's corona then extends out until the pressure of the coronal gas exceeds that of the magnetic field confining it, causing the field to open up and release the gas into the stellar wind. For the lower mass stars, however, whose coronae extend to distances greater than the corotation radius, the presence of a disc extending in as far as the corotation radius may disrupt this field. If this disruption is extreme, the presence of a disc may alter the structure of the stellar corona by shearing those field lines that pass through it, causing them to become open and therefore allowing coronal gas to escape in a wind (Lynden-Bell & Boily 1994; Lovelace, Romanova & Bisnovatyi-Kogan 1995). We refer to this as an *active* disc. This process is likely to reduce the overall X-ray EM, since it converts closed field lines that could contain hot X-ray emitting coronal gas into wind-bearing open field lines that will be dark in X-rays. This effectively places an upper limit on the size of the corona, since closed field lines cannot extend beyond the corotation radius. This would have the greatest impact on the lower mass stars whose coronae are naturally more extended because of their lower surface gravity. The X-ray emission from stars whose coronae did not extend as far as the corotation radius would be affected much less severely.

We therefore take the extent of the corona to have a maximum value of the location of the inner edge of the disc which we take to be at the corotation radius. We then calculate the EM of the gas contained in each stellar corona for a range of values of both the mean magnetic field at the stellar surface and the base pressure of the corona. We show in Table 1 the values of the base gas and magnetic pressure that give the minimum value of D [as defined by (6)] and show in Fig. 6 both the observed and the calculated EMs at these best-fitting values. The presence of an active disc clearly gives a rather better fit to the EMs at both the temperature ranges. This is mainly because of the lower mass stars which have coronae that extend beyond the corotation radius and whose EM is suppressed by the action of the disc stripping the corona. As a result, these stars have a lower EM than would be produced with a passive disc and so the slope of the fitted line is larger and closer to that found for the observed EMs. While the calculated densities (as shown in Fig. 4) are still lower than the observed ones, they are a little higher than if the disc is assumed to be passive and the slope of their variation with mass is greater. This is because the best-fitting value of the base pressure (and hence the base density) is higher for an active disc where the typically smaller sizes of the stellar coronae require higher densities to match the observed EMs. The lower temperature coronae with the smaller scaleheights are less affected by the presence of the disc and their density increase is typically less when an active disc is present.

2.3 Surface hotspots

Observations of magnetic fields on T Tauri stars and modelling of accretion signatures suggest that the fraction of the surface area of the star that is covered in accreting hotspots is very small, of the order of a few per cent (Muzerolle et al. 2003; Calvet et al. 2004; Valenti & Johns-Krull 2004; Muzerolle et al. 2005; Symington et al. 2005). We can place an upper limit on this by determining which field lines (in a corona whose size is limited only by pressure balance) would intersect the disc. Some subset of these field lines will be capable of supporting an accretion flow. We can determine this surface area fraction F by calculating the area of the two annuli on the stellar surface that lie between $\Theta_{\rm m}$ (the footpoint of the last closed field line) and $\Theta_{\rm KCR}$ (the footpoint of the field line that passes through the corotation radius). As a fraction of the total stellar surface area this gives

$$F = \cos\Theta_{\rm m} - \cos\Theta_{\rm KCR}. \quad (8)$$

This fraction is shown in Fig. 7 as a function of the coronal extent. If the corona does not extend out as far as the inner edge of the disc, then only those open-field lines that pass close to the equator will intersect the disc. Since these are likely to come from the polar regions, their area coverage at the stellar surface is very small. For those coronae that do extend beyond the inner edge of the disc, the area of the surface covered by those field lines that cross the disc depends on both the value of the corotation radius and also the maximum extent of the corona as determined by pressure balance. This can be seen from (4) since, if the stellar radius is sufficiently small compared to either the corotation radius or the maximum extent ($r_{\rm m}$) of the corona,

$$F \approx \frac{r_\star}{r_{\rm KCR}} - \frac{r_\star}{r_{\rm m}}. \quad (9)$$

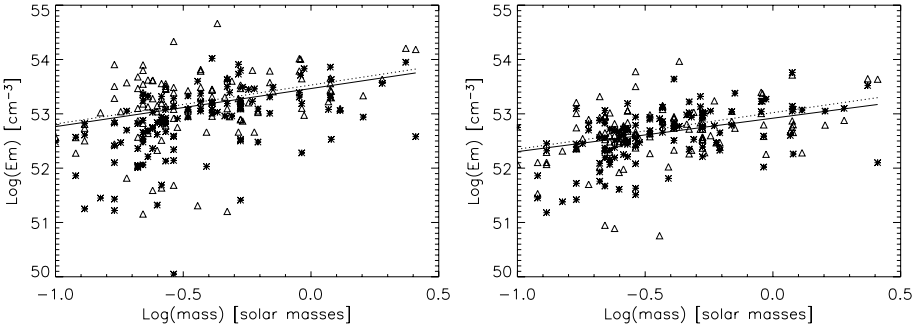

Figure 6. EMs for both the high-temperature (left-hand panel) and low-temperature (right-hand panel) ranges from the COUP sample. Crosses show the observed values while triangles show the values calculated for a dipole field with values of the base magnetic and plasma pressures that give the best fit to the data. We assume that each star has an *active* disc in the sense that the maximum extent of the corona is limited by the inner edge of the disc which is assumed to be at the corotation radius. The solid line is the best fit to the calculated values, while the dotted line is the best fit to the observed values, assuming the errors quoted for the values of log(EM).

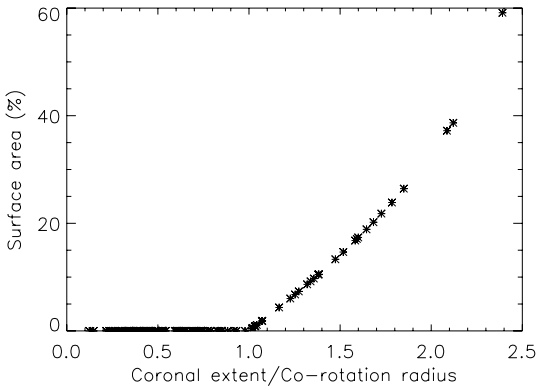

Figure 7. Crosses show the upper limit to the fraction of the stellar surface area that is covered in field lines that pass through the disc. A dipole field has been assumed.

This suggests that it is the lower mass stars with their more extended coronae that should show the largest hotspots.

It seems unlikely, however, that T Tauri stars will have simple aligned dipolar fields. The observations of significant rotational modulation of the X-ray emission from many of the stars in the COUP sample are a clear indication that their fields are more complex than a simple dipole. The pre-dominance of a period for the X-ray emission that is equal to (or half) that of the photometric period suggests the presence of either one dominant region of X-ray emission on the stellar surface or two at opposite longitudes. This is very similar to the predictions of the X-ray rotational modulation for AB Dor based on extrapolation of surface fields determined from Zeeman–Doppler imaging (Jardine et al. 2002a,b). These extrapolations show that the large-scale field of AB Dor resembles a tilted dipole, giving (in addition to many small-scale bright regions) two dominant bright regions at opposite longitudes. The latitudes of these bright regions can be related (crudely) to the tilt of this large-scale dipole. Depending on the stellar inclination one or both may be visible. We therefore explore the impact on the X-ray emission from these T Tauri stars that a field with a realistic degree of complexity might have.

3 FIELDS WITH A REALISTIC DEGREE OF COMPLEXITY

Although the observations to date suggest that T Tauri stars have fields that are more complex than a simple dipole, we do not as yet have any direct observations of the detailed geometry of the field. We therefore use fields extrapolated from surface magnetograms of two young solar-like stars, AB Dor (period 0.514 d) and LQ Hya (period 1.6 d) that have been obtained using Zeeman–Doppler imaging (Donati & Collier Cameron 1997; Donati et al. 1997, 1999, 2003). This allows us to determine the influence of field complexity and to assess the effect that this might have on our results based on simple dipolar fields. Since the rotation axes of both of these stars are inclined to the observer, only one hemisphere can be imaged reliably. In order to provide a realistic surface map for the hidden hemisphere, we use a map taken from another year. Thus, for the first map we use magnetograms of AB Dor generated from data acquired in 1995 and 1996 December, and for the second map we use magnetograms of LQ Hya generated from data acquired in 1993 and 2001 December. The coronal fields are extrapolated from these using the 'Potential Field Source Surface' method originally developed by Altschuler & Newkirk (1969) for extrapolating the Sun's coronal field from solar magnetograms. We use a code originally developed by van Ballegooijen, Cartledge & Priest (1998). Since the method has been described in Jardine et al. (2002a), we provide only an outline here. Briefly, we write the magnetic field $\boldsymbol{B}$ in terms of a flux function Ψ such that $\boldsymbol{B} = -\nabla\Psi$ and the condition that the field is potential ($\nabla \times \boldsymbol{B} = 0$) is satisfied automatically. The condition that the field is divergence-free then reduces to Laplace's equation $\nabla^2\Psi = 0$ with solution in spherical coordinates (r, θ, ϕ)

$$\Psi = \sum_{l=1}^{N} \sum_{m=-l}^{l} \left[a_{lm} r^{l} + b_{lm} r^{-(l+1)}\right] P_{lm}(\theta) \mathrm{e}^{\mathrm{i}m\phi}, \tag{10}$$

where the associated Legendre functions are denoted by P_{lm}. The coefficients a_{lm} and b_{lm} are determined by imposing the radial field at the surface from the Zeeman–Doppler maps and by assuming that at some height R_s above the surface (known as the *source surface*) the field becomes radial and hence $B_\theta(R_s) = 0$. This second condition models the effect of the plasma pressure in the corona pulling open-field lines to form a stellar wind.

For rapidly rotating solar-like stars, we can use the observed locations of the large slingshot prominences that typically form in their coronae to estimate the radii at which the corona must still be closed. For T Tauri stars, however, we do not have this option. As a fairly conservative estimate we choose to take the radial distance at which a *dipolar* field (of the same average field strength) would remain closed. We choose the dipolar field as it gives the greatest coronal extent (since of all the possible multipolar components, the dipolar falls off most slowly with radial distance). If this maximum extent exceeds the corotation radius, we set it to be the corotation radius instead.

We determine the pressure at every point by calculating the path of the field line through that point and solving hydrostatic equilibrium along that path. Once again, we set the gas pressure at the base of the field line to be proportional to the magnetic pressure there, noting, however, that now the base pressure varies across the stellar surface. By varying the constant of proportionality K we can raise or lower the overall level of the gas pressure. If along any field line we find that the gas pressure exceeds the magnetic pressure, we assume that the field line should have been opened up by the gas pressure and so we set $p = 0$.

We assume that the disc occupies a range of latitudes extending some 10° above and below the equator. We do not set the location of the inner edge of the disc, but allow it to adjust locally to the structure of the magnetic field at each latitude and longitude. We therefore assume that the disc extends in towards the surface of the star until it reaches the first field line along which (i) the gas pressure is less than the magnetic pressure everywhere along the field line, and (ii) the net gravitational force at the point where the field line passes through the disc acts inward towards the star. We assume that this first field line carries all the accreting material from that particular latitude and longitude and that it shields any field lines interior to it. Figs 8 and 9 show the structure of these accreting field lines, examples of the closed field lines that could contain hot coronal gas and X-ray images from the same perspective.

Of the two free parameters, one (the flux density or field strength) is determined by the surface magnetograms. As before, the other parameter is the constant of proportionality K that determines the gas pressure at the base of each field line. For the dipole field, we chose for simplicity to have a uniform p_0 based on the average field strength $\langle|B|\rangle$. For these complex fields, however, the base magnetic

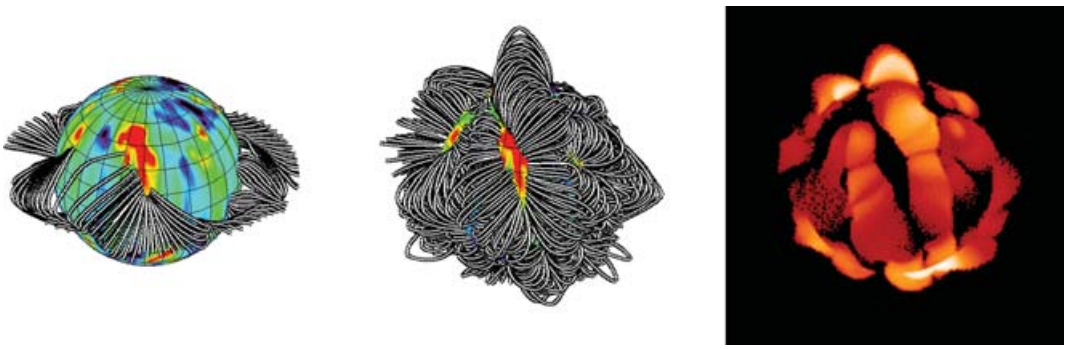

Figure 8. Calculated coronal structure based on an example surface magnetic field distribution for one of the lower mass stars (shown as a circle in Fig. 5) where it is the presence of the disc that is primarily limiting the extent of the corona. In this example, the stellar mass is 0.15 $M_\odot$, the radius is 4.02 $R_\odot$, the rotation period is 17.91 d and the natural extent of the corona (in the absence of a disc) would be at most 1.58 times the corotation radius. The left-hand panel shows the field lines that could support an accretion flow, drawn from the inner edge of the accretion disc which is situated at the corotation radius. The middle panel shows examples of the field lines that are closed and contain X-ray emitting gas and the right-hand panel shows the corresponding structure of the X-ray corona.

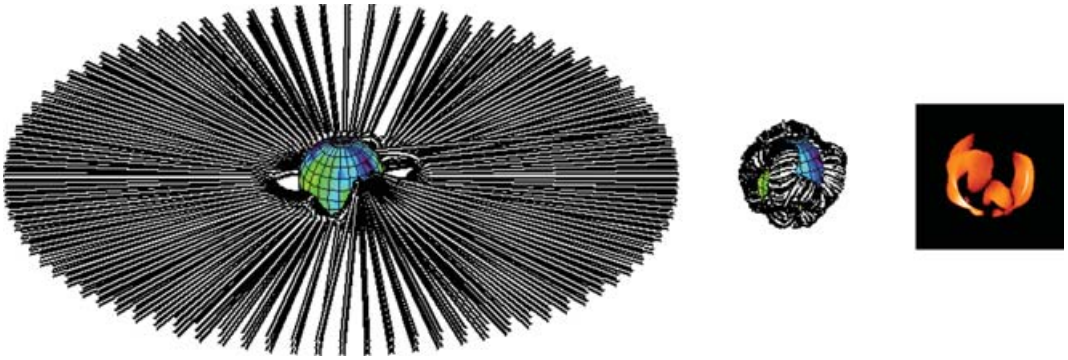

Figure 9. Calculated coronal structure based on an example surface magnetic field distribution for one of the higher mass stars (shown as a square in Fig. 5) where it is the pressure of the hot coronal gas that is primarily limiting the extent of the corona. In this example, the stellar mass is 2.57 $M_\odot$, the radius is 1.74 $R_\odot$, the rotation period is 1.38 d and the natural extent of the corona (in the absence of a disc) would be at most only 0.26 times the corotation radius. The left-hand panel shows the field lines that could support an accretion flow, drawn from the inner edge of the accretion disc which is situated at the corotation radius. The middle panel shows examples of the field lines that are closed and contain X-ray emitting gas and the right-hand panel shows the corresponding structure of the X-ray corona.

Table 2. This shows, for two example field structures with a realistic degree of complexity, the average field strength $B_0 = \langle |B| \rangle$ at the base of the corona and the corresponding gas pressure $p_0 = KB_0^2$. By fitting relationships of the form (EM) $\propto M_\star^a$ and $\bar{n}_e \propto M_\star^b$ to the calculated values of the EMs and densities, we have determined the values of a and b.

	AB Dor-like		LQ Hya-like	
T	High	Low	High	Low
$\langle \|B\| \rangle$ (G)	143	143	143	143
p_0 (dyne cm^{-2})	3.6	0.2	13.2	0.9
a	0.55	0.53	0.54	0.53
b	−0.05	−0.11	−0.06	−0.12

pressure can vary significantly across the surface and as a result, so can the base gas pressure. In Table 2, therefore, it should be noted that the value of $p_0 = K \langle |B| \rangle^2$ is just the value based on the average value of $\langle |B| \rangle$.

We can therefore, for each of the two example field structures, determine which value of K gives the best fit to the EMs from the COUP survey (see Fig. 10). We show in Fig. 11 the calculated EMs superimposed on the observed EMs. As can be seen from Table 2 the slopes for these calculated values are shallower than those for the observed EMs, but the values for the two field structures are remarkably similar.

There is more of a variation to be found in the densities (see Fig. 12). For the dipole field, densities of around 0.4×10^{10} cm^{-3} are typical for the high-temperature range. For these more complex fields, however, the densities are almost an order of magnitude higher (2.5×10^{10} cm^{-3}). The slopes are also less than for the active disc with a dipolar field. This is probably because the more compact fields can support a higher density, but they do not extend out as far as the dipolar fields and so they are less affected by the presence of a disc.

With these more complex fields, we would expect to find hotspots that are in different surface locations to those for a dipole field and that are perhaps different in size. Fig. 13 shows the fraction of the stellar surface area that is covered in field lines that pass through the inner edge of the disc. For the higher mass stars whose coronae do not reach out to the disc, the field lines that reach the disc are open and radial. Variations in the position of the corotation radius then have little effect in determining which field lines pass through

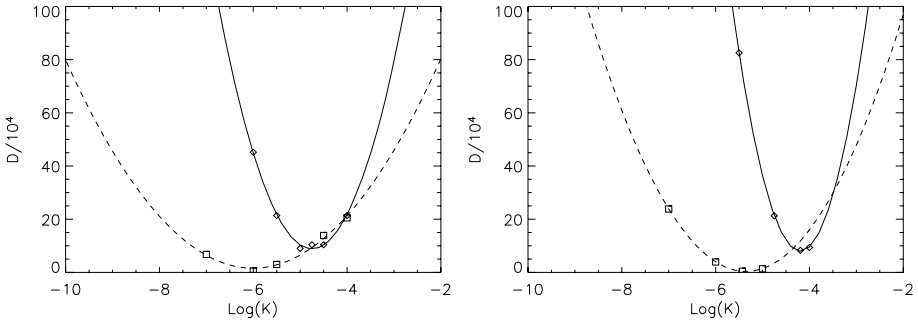

Figure 10. Variation of D (a measure of the goodness of fit to the data) with the base pressure for the field structure shown in Fig. 8 (left-hand panel) and for the field structure shown in Fig. 9 (right-hand panel). The solid lines denote the higher temperature coronae, and the dashed line the lower temperature coronae.

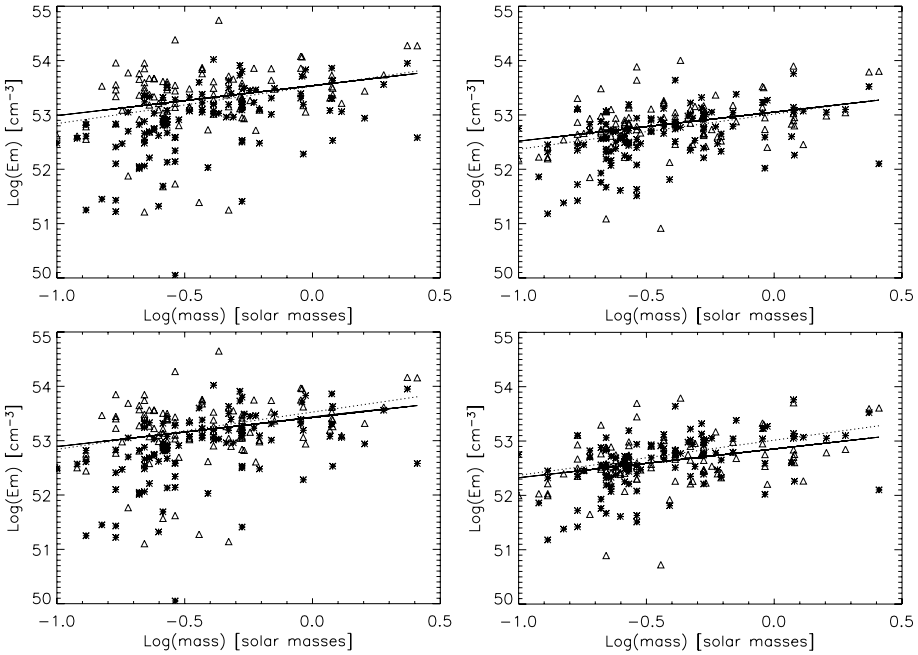

Figure 11. Observed EMs for both the low-temperature (left-hand panel) and high-temperature (right-hand panel) ranges from the COUP sample. The top panels refer to the field structure shown in Fig. 8 while the bottom panels refer to the field structure shown in Fig. 9. The solid line is the best fit to the calculated EMs, while the dotted line is the best fit to the observed EMs.

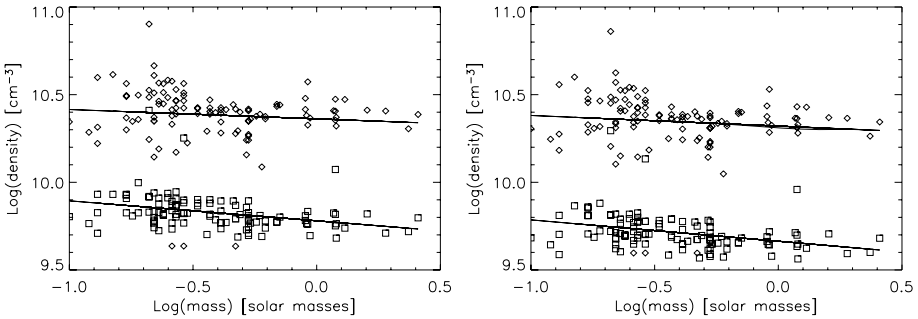

Figure 12. EM-weighted densities for both the high-temperature (diamonds) and low-temperature (squares) ranges from the COUP sample. The left-hand panel refers to the magnetic fields shown in Fig. 8 and the right-hand panel to the magnetic fields shown in Fig. 9.

the disc and so the fraction of accreting field lines varies little with stellar mass. For those lower mass stars whose coronae extend out beyond the corotation radius, the stellar magnetic field is still closed at the inner edge of the disc. Consequently, changes in the corotation radius can make large changes to whether a field line is accreting or not and so the surface area of hotspots shows a greater scatter. In either instance, however, the filling factor is low, in agreement with results from modelling of accretion signatures (Muzerolle et al. 2003; Calvet et al. 2004; Valenti & Johns-Krull 2004; Muzerolle et al. 2005; Symington et al. 2005).

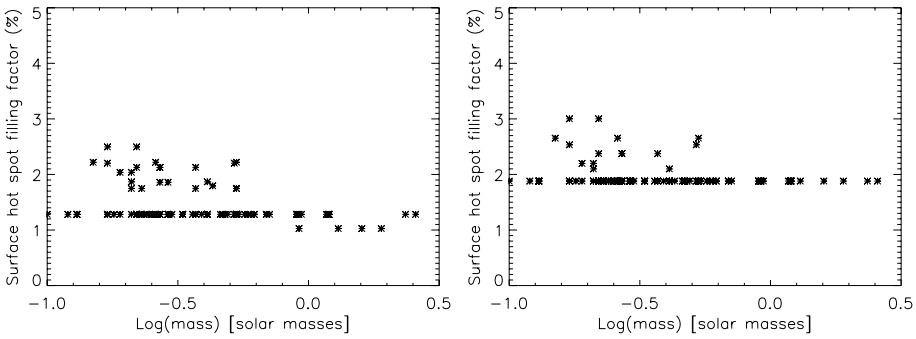

Figure 13. Surface-filling factor of hotspots for the magnetic fields shown in Fig. 8 (left-hand panel) and for the magnetic fields shown in Fig. 9 (right-hand panel).

4 SUMMARY AND DISCUSSION

We have shown in this paper that it is possible for a simple model to reproduce the observed variation with mass of the X-ray EM of T Tauri stars. This variation is due to the restriction in the size of the stellar corona that results either from the pressure of the hot coronal gas in opening up the magnetic field lines, or from the shearing effect of a circumstellar disc. The ratio of the pressure scaleheight to the corotation radius (a reasonable estimate of the location of the inner edge of an accretion disc) scales as $\Lambda/R_{\rm KCR} \propto M_\star^{-2}$ for a polytropic star. Hence, lower mass stars are more likely to have coronae that reach the inner edge of any accretion disc present and so their coronal extent will be set by the corotation radius. Higher mass stars have coronae that may not extend as far as the corotation radius and so their coronal extent is set simply by the ability of the magnetic field to contain the gas. For these stars, accretion will occur principally along open, nearly radial magnetic field lines.

Even in the absence of a disc, the variation of the extent of the corona will produce a drop in the X-ray EM with decreasing stellar mass. This process of *coronal stripping* has already been shown to reproduce the observed variation with rotation rate of both the magnitude and rotational modulation of the X-ray EMs of main-sequence stars (Unruh & Jardine 1997; Jardine & Unruh 1999; Jardine 2004). The stars in the COUP sample appear to lie in the saturated or supersaturated part of the rotation–activity relation (i.e. where X-ray EM is independent of rotation rate or even falling with increasing rotation rate). However, their EMs are slightly lower than their main-sequence counterparts and they show a greater scatter. Preibisch et al. (2005) have examined this question of the overall suppression of the X-ray emission. They divide the sample of stars into those that show some indication of the presence of a disc (i.e. an infrared excess) but no apparent signatures of active accretion (as measured by the width of the Hα line) and those that show indications of both. The main contributors to the drop in X-ray emission appear to be those stars that show signs of active accretion and for which there is therefore clear evidence that their discs are interacting with the stellar magnetic field. Stars lacking this clear signature of disc interaction appear to show a level of X-ray emission that is similar to their saturated or supersaturated main-sequence counterparts. This is consistent with our model which predicts that all stars will show a drop in emission with decreasing mass due to the pressure stripping of their coronae, but that in those stars where a disc is actively interacting with and distorting the stellar magnetic field, this drop in emission will be further enhanced. Preibisch et al. (2005) also noted that the large scatter in X-ray emission is most pronounced in the actively accreting stars. This can be understood in terms of our model since in those stars where the disc is actively stripping the corona, the coronal extent depends on a further parameter, the rotation rate, since this determines the location of the corotation radius where the inner edge of the disc is most likely to be situated.

The observations of the strength of the magnetic field at the base of the accretion funnels and across the rest of the stellar surface (Valenti & Johns-Krull 2004; Symington et al. 2005) combined with the observation of significant X-ray rotational modulation in stars in the COUP sample (Flaccomio et al. 2005) have prompted us to investigate the importance of the nature of the stellar magnetic field. We have modelled the extent of the stellar corona, the X-ray EM and the density both for a simple dipole field and also for fields with a realistic degree of complexity. We do not yet know in detail the structure of T Tauri coronal fields, but we have used instead coronal magnetic fields extrapolated from surface magnetograms of young main-sequence stars. While we do not yet know if these capture the coronal structure of T Tauri stars, they allow us to explore the effect of a more compact field. This is important as dipole fields (the most commonly used example until now) fall off with height more slowly than any other type of field except a purely radial one. They therefore model the most extended type of field possible. Fields that are more complex are more compact: their field strengths decay with height more rapidly than a dipolar field and so they will typically be less extended than a dipole and consequently are likely to produce a higher density.

We find that the more complex fields do indeed produce more compact, higher density coronae, with densities in the range (2.5–0.6) $\times$ $10^{10}\,{\rm cm}^{-3}$ for coronae whose temperatures are set to the 'high' and 'low' temperatures in the COUP data base. These densities are nearly an order of magnitude higher than for a dipole field. The densities produced by different types of complex fields are relatively similar, with the main differences being the locations of the surface hotspots (where the accretion flows impact on the stellar surface) and their filling factors. In contrast to dipole fields where any accretion flow must reach the surface at the poles (thereby producing no rotational modulation), more complex fields can produce hotspots at lower latitudes. Mahdavi & Kenyon (1998) have modelled the locations of hotspots in dipole field that are tilted with respect to the rotation axis, but these can only provide one hotspot in each hemisphere, while more complex fields can produce many smaller hotspots at a range of latitudes and longitudes. We find filling factors are small (typically a few per cent) in agreement with predictions made from modelling accretion signatures (Muzerolle et al. 2003; Calvet et al. 2004; Valenti & Johns-Krull 2004; Muzerolle et al. 2005; Symington et al. 2005).

We have also calculated the form of the relationship (EM) $\propto M_\star^a$ based on the published stellar masses, radii, rotation rates and coronal temperatures for the COUP stars (Getman et al. 2005). For the higher temperature range in the COUP sample, the observed EMs (allowing for the published errors) give a value of $a = 0.68$. If we assume that all stars have either no disc present, or only a *passive* disc that does not distort the stellar corona, we find a value of $a = 0.34$ for a dipole field, compared with $a = 0.70$ if we assume that all stars have an *active* disc that distorts any stellar corona that extends as far as the inner edge of the disc (which is assumed to be at the corotation radius). If we assume a more complex field geometry this value drops to $a = 0.55$ if the stellar discs are assumed to be active. A similar result is found for the low-temperature component. Thus, the presence of discs capable of distorting those stellar coronae that extend beyond the corotation radius seems to be necessary to explain the slope of the observed variation with mass of the X-ray EM. The degree of complexity of the field has a smaller effect on the overall X-ray emission, but it does have a significant effect on the densities. Assuming that all stars have dipole fields gives densities much lower than those derived from observations of flares (Favata et al. 2005), while the assumption of a more complex field geometry gives densities comparable to the published values. These results taken together suggest that the true T Tauri stellar fields may be more extended than those of the main-sequence counterparts, but not by as much as a purely dipole field. They may simply have a dipolar component that is somewhat stronger than in the main-sequence stars.

In summary, we have shown that a simple model (which reproduces the X-ray activity–rotation relation for main-sequence stars) can explain the variation of X-ray EM with stellar mass observed in the COUP survey, if we allow for the presence of an accretion disc which will limit the size of any stellar corona that reaches out to its inner edge.

ACKNOWLEDGMENT

The authors would like to thank Aad van Ballegooijen who wrote the original version of the field-extrapolation software.

REFERENCES

Altschuler M. D., Newkirk Jr. G., 1969, Solar Phys., 9, 131
Calvet N., Muzerolle J., Briceño C., Hernández J., Hartmann L., Saucedo J. L., Gordon K. D., 2004, AJ, 128, 1294
Donati J.-F., Collier Cameron A., 1997, MNRAS, 291, 1
Donati J.-F., Semel M., Carter B. D., Rees D. E., Collier Cameron A., 1997, MNRAS, 291, 658
Donati J.-F., Collier Cameron A., Hussain G., Semel M., 1999, MNRAS, 302, 437
Donati J.-F. et al., 2003, MNRAS, 345, 1145
Favata F., Flaccomio E., Reale F., Micela G., Sciortino S., Shang H., Stassun K. G., Feigelson E. D., 2005, ApJS, 160, 469
Flaccomio E., Micela G., Sciortino S., Feigelson E. D., Herbst W., Favata F., Harnden F. R., Vrtilek S. D., 2005, ApJS, 160, 450
Getman K. V. et al., 2005, ApJS, 160, 319
Güdel M., 2004, A&AR, 12, 71
Guenther E. W., Lehmann H., Emerson J. P., Staude J., 1999, A&A, 341, 768
Ivanova N., Taam R. E., 2003, ApJ, 599, 516
Jardine M., Unruh Y., 1999, A&A, 346, 883
Jardine M., Collier Cameron A., Donati J.-F., 2002a, MNRAS, 333, 339
Jardine M., Wood K., Collier Cameron A., Donati J.-F., Mackay D. H., 2002b, MNRAS, 336, 1364
Jardine M., 2004, A&A, 414, L5
Johns-Krull C. M., Valenti J. A., Koresko C., 1999, ApJ, 516, 900
Johns-Krull C. M., Valenti J. A., Saar S. H., 2004, ApJ, 617, 1204
Lovelace R. V. E., Romanova M. M., Bisnovatyi-Kogan G. S., 1995, MNRAS, 275, 244
Lynden-Bell D., Boily C., 1994, MNRAS, 267, 146
Mahdavi A., Kenyon S. J., 1998, ApJ, 497, 342
Muzerolle J., Hillenbrand L., Calvet N., Briceño C., Hartmann L., 2003, ApJ, 592, 266
Muzerolle J., Luhman K. L., Briceño C., Hartmann L., Calvet N., 2005, ApJ, 625, 906
Preibisch T. et al., 2005, ApJS, 160, 401
Symington N. H., Harries T. J., Kurosawa R., Naylor T., 2005, MNRAS, 358, 977
Unruh Y., Jardine M., 1997, A&A, 321, 177
Valenti J. A., Johns-Krull C. M., 2004, Ap&SS, 292, 619
van Ballegooijen A., Cartledge N., Priest E., 1998, ApJ, 501, 866

APPENDIX A

In deriving expressions for the variation of the EM and density with radial distance from the star, we begin with (3). If we scale all distances to a stellar radius, we can write

$$p(r,\theta) = p_\star(1,\theta)\exp\left[\Phi_{\rm g}\left(\frac{1}{r}-1\right)+\Phi_{\rm c}\sin^2\theta(r^2-1)\right], \quad \text{(A1)}$$

where $p_\star(1,\theta)$ is the pressure distribution across the stellar surface and

$$\Phi_{\rm g} = \frac{GM/r_\star}{k_{\rm B}T/m}, \quad \text{(A2)}$$

$$\Phi_{\rm c} = \frac{\omega^2 r_\star^2/2}{k_{\rm B}T/m}, \quad \text{(A3)}$$

are the surface ratios of gravitational and centrifugal energies to the thermal energy. The EM $= \int n_{\rm e}^2\,{\rm d}V$ is then

$$\begin{aligned}{\rm EM} = {} & \frac{4\pi r_\star^2}{(k_{\rm B}T)^2},\\ & \int_{\theta=\Theta_{\rm m}}^{\theta=\pi/2} p_\star^2(1,\theta)\exp\left[-2\Phi_{\rm c}\cos^2\theta(r^2-1)\sin\theta\,{\rm d}\theta\right],\\ & \int_{r=1}^{r=r_{\rm m}} r^2\exp\left[2\Phi_{\rm g}\left(\frac{1}{r}-1\right)+2\Phi_{\rm c}(r^2-1)\right]{\rm d}r. \end{aligned} \quad \text{(A4)}$$

If we now use the substitution $\mu = \cos\theta$ such that $\mu_{\rm m} = \cos\Theta_{\rm m} = (1 - r/r_{\rm m})^{1/2}$ then the θ-integral can be written as

$$\int_0^{\mu_{\rm m}} p_\star^2(1,\theta)\exp\left[-2\Phi_{\rm c}\mu^2(r^2-1)\right]{\rm d}\mu, \quad \text{(A5)}$$

which, on using the substitution $t = [2\Phi_{\rm c}(r^2-1)]^{1/2}\,\mu$ gives

$$\frac{1}{2\Phi_{\rm c}(r^2-1)^{1/2}}\int_0^{t_{\rm m}} p_\star^2(1,\theta){\rm e}^{-t^2}{\rm d}t, \quad \text{(A6)}$$

where $t_{\rm m} = [2\Phi_{\rm c}(r^2-1)]^{1/2}\,(1 - r/r_{\rm m})^{1/2}$. If we now assume that the pressure is uniform over the stellar surface, we obtain the

following expression for the EM as a function of r:

$$\mathrm{EM}(r) = \sqrt{\frac{2\pi^3}{\Phi_\mathrm{c}}}\frac{r_\star^3 p_\star^2}{(k_\mathrm{B}T)^2}, \int_{r=1}^{r=r_\mathrm{m}} \frac{r^2}{(r^2-1)^{1/2}}\mathrm{erf}\left[2\Phi_\mathrm{c}(r^2-1)\left(1-\frac{r}{r_\mathrm{m}}\right)\right]^{1/2}, \exp\left[2\Phi_\mathrm{g}\left(\frac{1}{r}-1\right)2\Phi_\mathrm{c}(r^2-1)\right]\mathrm{d}r. \quad \text{(A7)}$$

We can, in a similar way, obtain an expression for the EM-weighted density $\bar{n}_\mathrm{e}(r) = \int n_\mathrm{e}^3\,\mathrm{d}V / \int n_\mathrm{e}^2\,\mathrm{d}V$.

$$\bar{n}_\mathrm{e}(r) = \frac{1}{\mathrm{EM}(r)}\sqrt{\frac{\pi^3}{3\Phi_\mathrm{c}}}\frac{2r_\star^3 p_\star^3}{(k_\mathrm{B}T)^3}, \int_{r=1}^{r=r_\mathrm{m}} \frac{r^2}{(r^2-1)^{1/2}}\mathrm{erf}\left[3\Phi_\mathrm{c}(r^2-1)\left(1-\frac{r}{r_\mathrm{m}}\right)\right]^{1/2}, \exp\left[3\Phi_\mathrm{g}\left(\frac{1}{r}-1\right)3\Phi_\mathrm{c}(r^2-1)\right]\mathrm{d}r, \quad \text{(A8)}$$

where we remind the reader that all distances r have been scaled to a stellar radius.

This paper has been typeset from a TEX/LATEX file prepared by the author.